Title

4D Flow MR Imaging to Improve Microwave Ablation Prediction Models: A Feasibility Study in an In Vivo Porcine Liver

Journal

Journal of Vascular and Interventional Radiology, 31(10)

ISSN

1051-0443

Authors

Chiang, Jason
Loecher, Michael
Moulin, Kevin
et al.

Publication Date

2020-10-01

DOI

10.1016/j.jvir.2019.11.034

Peer reviewed

HHS Public Access

Author manuscript

J Vasc Interv Radiol. Author manuscript; available in PMC 2021 October 01.

Published in final edited form as:

J Vasc Interv Radiol. 2020 October ; 31(10): 1691–1696.e1. doi:10.1016/j.jvir.2019.11.034.

4D flow MR imaging to improve microwave ablation prediction models: A feasibility study in an in vivo porcine liver

Jason Chiang, MD, PhD[1], **Michael Loecher, PhD**[2], **Kevin Moulin, PhD**[2], **Maria Franca Meloni, MD**[3], **Steven Raman, MD**[1], **Justin P. McWilliams, MD**[1], **Daniel Ennis, PhD**[2], **Edward W. Lee, MD, PhD**[1]

[1]Department of Radiology, Ronald Reagan UCLA Medical Center, Los Angeles, CA, USA

[2]Department of Radiology, Stanford University School of Medicine, Stanford, CA, USA

[3]Department of Interventional Ultrasound, Casa di Cura Igea, Milan, Italy

Abstract

Purpose—To characterize the effect of hepatic vessel flow using 4D flow MRI and correlate their effect on microwave ablation volumes in an in vivo non-cirrhotic porcine liver model.

Materials and Methods—Microwave ablation antennas were placed under ultrasound guidance in each liver lobe of swine (n=3 in each animal) for a total of nine ablations. Pre- and post-ablation 4D flow MRI were acquired to quantify flow changes in the hepatic vasculature. Flow measurements, along with encompassed vessel size and vessel-antenna spacing were then correlated with ablation volume from segmented MR images.

Results—The linear regression model demonstrated that the pre-ablation measurement of encompassed hepatic vein size ($\beta = -0.80 \pm 0.25$, 95% CI: [−1.15, −0.22]; p=0.02) was significantly correlated to final ablation zone volume. The addition of hepatic vein flow rate found via 4D flow MRI ($\beta = -0.83 \pm 0.65$, 95% CI: [−2.50, 0.84]; p=0.26), and distance from antenna to hepatic vein ($\beta = 0.26 \pm 0.26$, 95% CI: [−0.40, 0.92]; p=0.36) improved the model accuracy but not significantly so (multivariate adjusted $R^2 = 0.70$ vs univariate (vessel size) adjusted $R^2 = 0.63$, p=0.24).

Conclusions—Hepatic vein size in an encompassed ablation zone was found to be significantly correlated with final ablation zone volume. While the univariate 4D flow MRI-acquired measurements alone was not found to be statistically significant, its addition to hepatic vein size improved the accuracy of the ablation volume regression model. Pre-ablation 4D flow MRI of the liver may assist in prospectively optimizing thermal ablation treatment.

Please address editorial correspondence to: Jason Chiang, MD, PhD, cjchiang@mednet.ucla.edu, UCLA Ronald Reagan Medical Center, 757 Westwood Plaza, Suite 1638, Los Angeles, CA 90095.

Disclosures:

J.C. has intellectual property relating to microwave ablation technology and receives licensing fees through the Wisconsin Alumni Research Foundation. J.M. and S.R. received speaker fees from Ethicon Neuwave Medical Inc.

INTRODUCTION

Microwave ablation (MWA) is increasingly utilized in place of radiofrequency (RF) ablation due to higher heating efficiency and ability to more consistently deliver energy into targeted tumor tissue (1). However, as with all heat-based ablation modalities, microwave ablations are also limited by both perfusion-mediated and vascular cooling. This phenomenon, known as the “heat-sink effect” is characterized by the surrounding blood flow that transports heat away from the ablation zone(2). Consequently, the heat-sink effect has been associated with decreased treatment efficacy and increased risk for local tumor progression (3–5).

Multiple efforts have sought to optimize MWA energy delivery into tissue to overcome the heat-sink effect, but there exist only limited studies that characterize the effect of blood flow on the ablation zone itself. Computational models show that larger amounts of flow either in a single vessel or through liver parenchyma would siphon more heat away from an ablation zone (6). However, validation studies using phantom and *in-vivo* liver flow models are limited by the size and spatial resolution of commercially available flow and pressure sensors (6–8). Consequentially, researchers have relied on overly-simplified vessel models that may not capture the true hemodynamic profile of an entire liver.

Recent developments in MRI acquisitions and computational flow dynamics have introduced new techniques to further characterize the hemodynamics of the liver. 4D flow MR is a 3D phase-contrast MRI with three-directional flow encoding that can evaluate not only vascular anatomy but also blood flow and velocity (9–11). The benefit of 4D flow relative to ultrasound Doppler is that it can provide comprehensive volumetric flow throughout the liver instead of just peak through-plane velocity at a single point in time. Using 4D flow MRI, physicians have been able to investigate liver pathologies such as portal hypertension as well as monitor liver hemodynamics after interventions such as TIPS or liver transplant (10,12).

Quantifying the liver flow dynamics before and after an ablation procedure can provide critical information about how blood flow interacts with ablation zones, particularly with perivascular tumors that are most susceptible to the heat-sink effect. The purpose of this study was to characterize the effect of hepatic blood flow on microwave ablation volumes in an in vivo porcine liver model using 4D flow MRI.

MATERIALS AND METHODS

All studies were performed with approval from the local institution’s Animal Care and Use Committee and in accordance to the National Research Council Guide for the Care and Use of Laboratory Animals guideline (13). Domestic swine (n=3; female Yorkshire swine weighing 30–40 kg; median 37 kg) were sedated with intramuscular tiletamine hydrochloride–zolazepam hydrochloride (7 mg/kg, Telazol, Fort Dodge, IA) and xylazine hydrochloride (2.2 mg/kg, Xyla-Ject, Phoenix Pharmaceutical, St. Joseph, MO) and anesthetized with inhaled 1.0–2.0% isoflurane (Halocarbon Laboratories, River Edge, NJ) during the imaging and ablation procedures.

The 4D flow MRI parameters included: retrospectively gated stack-of-spirals trajectory, TE/TR = 2.1ms/5.3ms, resolution = 1×1×2 mm, FOV = 320×320×80 mm, Venc = 60 cm/s,

scan time = 12 minutes. The Venc value of 60 cm/sec was used with a multidirectional high-moment acquisition (MDHM), which allowed unwrapping up to 180 cm/sec, values that were expected to fully capture the range of velocities seen in hepatic arteries(14). Pre-ablation angiograms were created from the 4D-flow MRI data, which were then subsequently used to make high-resolution mesh of the vascular contours of the *in vivo* porcine liver anatomy. After the pre-ablation procedure, the porcine subject was removed from the MRI bore and moved to a procedural room where the microwave ablation procedure took place.

Microwave ablations were performed using a 2.45 GHz ablation system and a single 17-gauge antenna (Certus 140 and PR-15, Neuwave Medical Inc, Madison WI). A single ablation (65 W for 5 minutes) was performed in each liver lobe (n=3 for each animal: left lateral, left medial and right medial, for a total of 9 ablations). A single lobe was left open to minimize the risk liver infarction and to maintain liver reserves during the ablation procedure and scans. Antennas were strategically placed under ultrasound guidance to be within 1 cm of nearby hepatic vessels. After ablation zones were created, the porcine subject was placed back into the MRI bore to undergo the post-ablation 4D flow MRI. Ablation zones that were abutting or encased (completely surrounding) targeted vessels of interest were segmented on a non-contrast T1-weighted image to create a volume measurement. Post-processing of the velocity data from phase contrast scans were performed on commercially-available software (Ensight; Computational Engineering International, Apex, NC). Sample images of the 4D flow MRI, segmentation and co-registration of the ablation volumes are shown in Figure 1.

After the procedure, the swine were euthanized with an intravenous dose of pentobarbital sodium and phenytoin sodium (Beuthanasia-D, Schering-Plough, Kenilworth, NJ) and their respective livers removed en-bloc. All animals survived until sacrifice after the post-ablation scan. Ablation zones were sectioned along the insertion tract of the antenna. Vessel thrombosis was confirmed on gross histology. The sections were photographed and stored as digital images. Standard ablation zone metrics (diameter and length) were measured on both gross pathology and used to validate the MRI ablation segmentation volumes.

Statistics

Pre- and post-ablation 4D-flow MRI measurements were acquired and compared via paired Student t-test. Thrombosed vessels, demonstrated by lack of flow on post-ablation 4D-flow MRI and confirmed on gross pathology, were compared between portal veins and hepatic veins via non-parametric McNemar's test. Multi-variate linear regression modeling was performed on the mean pre-ablation blood flow velocity (mL/sec) of both hepatic veins and portal veins, their respective sizes and distance to the emission point on the microwave antenna. In order to find the most accurate model that predicts the final ablation volume, a backwards stepwise model selection process was utilized. The metric for model optimization was based on the highest adjusted linear coefficient of determination R^2 for predicting ablation volume. Due to low sample size, the 95^{th} percentile confidence interval of each individual coefficient of determination was calculated using 1000 bootstrap samples with replacements. Variables that had the best fit were then selected out and analyzed via

regression modeling. P values < 0.05 were considered significant. All statistical analysis was performed with statistical software R (R version 3.5.2, Vienna, Austria).

RESULTS

Blood Flow data

A total of 6 segmental portal veins, 8 segmental hepatic veins and 3 proper hepatic arteries were visualized. Out of the vessels encompassed within ablation zones, 0/8 hepatic veins were thrombosed while 3/6 portal veins were thrombosed (p=0.21) (Figure 2). No hepatic arteries were thrombosed.

There was a significant decrease in hepatic vein flow from pre-ablation to post-ablation procedure (2.3 ± 0.7 vs 1.5 ±0.44 mL/sec respectively, p=0.006). There was a similar decrease in portal vein velocity (2.1 ± 0.9 vs 1.8 ±1.1 mL/sec, respectively, p=0.73) although this was not found to be statistically significant. Blood flow in portal veins found to be 0 mL/sec after ablation was a reflection of portal vein thrombosis and confirmed on gross pathology. Within hepatic arteries the blood flow decreased from pre-ablation to post-ablation (12.4 ±1.5 mL/sec vs 10.5 ± 0.4 mL/sec, p=0.39), although this decrease was also not significant. Segmental and subsegmental branches of the hepatic arteries were too small to perform accurate flow analysis.

Ablation zones in each liver lobe using 3D manual segmentation measured from 2.5 mL to 12.4 mL in volume. The multivariate regression model with hepatic veins showed the highest coefficient of determination (adjusted R^2 = 0.70, p=0.03) when utilizing pre-ablation hepatic vein size (β = −0.80±0.25, 95% CI: [−1.15, −0.22]; p=0.02), hepatic vein flow rate (β = −0.83 ± 0.65, 95% CI: [−2.50, 0.84]; p=0.26), and distance from antenna to hepatic vein (β = 0.26 ± 0.26, 95% CI: [−0.40, 0.92]; p=0.35). The bivariate regression model using hepatic vein size (β = −0.76 ± 0.25, 95% CI:[−1.37, −0.15]; p=0.02) and flow rate (β = −0.92 ± 0.64, 95% CI:[−2.50, 0.65]; p=0.18) had a similar adjusted linear regression model (adjusted R^2 = 0.69, p=0.01). When compared to univariate hepatic vein size, the adjusted R^2 in the model utilizing hepatic vein size, flow rate and vessel-antenna distance was higher, but not significantly so (adjusted R^2 = 0.70 vs 0.63, p=0.24). Univariate contributions from hepatic vein size and hepatic vein flow rate are plotted in Supplementary Figure 1. The regression model of pre-ablation vessel size, flow rates and vessel-antenna distance for portal veins was not significantly correlated to ablation zone size (p=0.71, 0.86 and 0.95, respectively).

Notably, the two largest ablation zones (10.5 and 12.4 mL) occurred in the presence of thrombosed portal veins. The smallest two ablation zones (2.5 and 2.6 mL) occurred in the presence of one or two patent hepatic veins encompassed within the ablation zone (Figure 3).

DISCUSSION

The results of our study demonstrated that quantitatively characterizing the hepatic vasculature in the liver prior to microwave ablations can improve correlation to final ablation

zone volume. Univariate hepatic vein size was significantly correlated with final ablation size, but univariate hepatic vein blood flow obtained via 4D flow MRI was not. However, the addition of hepatic vein blood flow improved the regression model. In particular, the combination of pre-ablation hepatic vein size, vessel-antenna spacing, and blood flow as characterized on 4D flow MRI had the highest correlation with final ablation zone volume. The regression analysis suggests that an increase in univariate hepatic vein diameter of 1.25 mm can lead to a 1 mL decrease in final ablation volume size, or approximately 25% less than that predicted in a non-perivascular ablation zone. Although not significant, the regression coefficients of the linear model of univariate hepatic vein blood flow suggests that increments of 0.8 mL/sec increases in blood flow is correlated with a 1 mL decrease in microwave ablation volume. Portal veins thrombosed at a higher rate compared to hepatic veins and consequently their associated flow rate and size were not well correlated to ablation zone volumes. While the hepatic arteries remained patent during the ablation and likely contributed to the heat-sink effect, their vessel sizes at the segmental and subsegmental branches were too small to be completely evaluated on 4D flow MRI. Globally, the microwave ablation zone resulted in a decrease in blood flow velocity in hepatic vasculature, although this was only found to be significant in hepatic veins.

The finding that hepatic vein size was significantly correlated with final microwave ablation volume is consistent with prior reports. In the Yu et al. study, the heat-sink effect was graded based on the amount of ablation zone invagination around an encompassed hepatic vein (5). This study expands on that conclusion by correlating hepatic vein size to final ablation zone volume, a more quantitative measurement. While univariate hepatic vein blood flow was not found to be statistically significant, the linear regression model to predict final ablation volume did improve when combining hepatic vein blood flow to hepatic vein size in perivascular ablation zones. Prior studies have demonstrated that millimeter sized vessels draw heat away from thermal ablation zones, limiting the efficacy of radiofrequency ablation(15). Utilizing microwave ablation has been associated with less heat-sink effect and has the theoretical advantages of more homogeneous heating in hepatic tissue (1). However, recent in vivo and in vitro studies have demonstrated that various vessel types may interact with heat differently (16). Hepatic veins are far more resistant to heat-induced vascular occlusion compared to portal veins and thus can act as a larger, more robust heat sink during thermal ablations (17). This result demonstrated the consequence of persistent heat sinks, with significantly smaller ablation zones in tissue that contain hepatic veins compared to portal veins.

Mapping out hepatic vascular anatomy and flow with 4D flow MRI offers potential advantages to thermal ablation treatment planning. The ability to map out the blood flow velocities *a priori* allows physicians to more accurately plan out the ablation treatment (i.e. energy and duration) and more effectively guide their antennas in the setting of liver tumors surrounded by high-flow hepatic vessels. For example, peri-vascular tumors that abut prominent hepatic veins may warrant more aggressive treatment requiring higher time-power settings or multiple antenna approach. Similarly, tumors that abut smaller portal veins with slower flow rates seen on 4D flow MRI may take a more conservative treatment strategy and minimize the risk for lobar infarct (18,19). 4D flow MRI also provides a volume flow rate that lends itself well to numerical modeling simulations (20,21). While ablation modeling

for treatment planning is still at its infancy, combining patient-specific anatomy with existing bioheat transfer models offers a potential solution to prospectively evaluating where the margins of a final ablation zone can be located.

There are some notable limitations to this study that may constrain the generalizability of this study. The *in vivo* porcine liver model did not have a tumor burden and lacked the associated vasculature changes in cirrhosis and portal hypertension that can be seen in primary liver malignancies. There are available tumor models such as the rabbit VX2 model or onco-pig model that may offer a more translatable model to clinical practice. Additional work using 4D flow MRI on one of these tumor models may reveal insight into how perivascular tumors may respond to locoregional therapies such as thermal ablation. Secondly, the study was limited by the spatial and temporal resolution of the 4D flow data, which only captured vessels down to the 2 mm size, thereby limiting evaluation of blood flow in segmental and subsegmental hepatic arteries. Slower blood flow values such as those seen in portal and hepatic veins were subject to high signal to noise ratio, potentially limiting the accuracy of our blood flow measurements. Finally, our sample size was low and subject to the confounding factors as noted above. However, this limitation is partially overcome by non-parametric boot-strapping techniques in order to estimate the regression coefficients and 95% percentile confidence intervals.

In conclusion, hepatic vein diameters within encompassed microwave ablation zones were found to be significantly correlated to the final ablation zone size. While the blood flow velocity data from 4D flow MRI alone was found to not be significantly correlated to the final ablation zone size, the blood flow velocity did improve the accuracy of the multivariate regression model for predicting the final ablation zone. Quantifying pre-ablation hepatic vein blood flow via 4D flow MRI can help physicians better predict the final size of the ablation zone and margin. Recognizing the presence and size of hepatic veins may warrant more aggressive treatment of perivascular tumors to minimize the risk of local tumor progression. 4D flow MRI can potentially be adopted into current surveillance guidelines for the rapidly growing liver malignancy population.

Supplementary Material

Refer to Web version on PubMed Central for supplementary material.

Acknowledgements

J.C. is supported through UCLA Department of Radiology Exploratory Research Grant and NIH CTSI Grant UL1TR001881.

References

1. Brace CL. Microwave tissue ablation: biophysics, technology, and applications. Crit Rev Biomed Eng. 2010;38(1):65–78. [PubMed: 21175404]
2. Ahmed M, Technology Assessment Committee of the Society of Interventional Radiology. Image-guided tumor ablation: standardization of terminology and reporting criteria--a 10-year update: supplement to the consensus document. J Vasc Interv Radiol JVIR. 2014 11;25(11):1706–8. [PubMed: 25442133]

3. Chiang J, Cristescu M, Lee MH, Moreland A, Hinshaw JL, Lee FT, et al. Effects of Microwave Ablation on Arterial and Venous Vasculature after Treatment of Hepatocellular Carcinoma. Radiology. 2016 6 3;152508.
4. Bhardwaj N, Dormer J, Ahmad F, Strickland AD, Gravante G, West K, et al. Microwave ablation of the liver: a description of lesion evolution over time and an investigation of the heat sink effect. Pathology (Phila). 2011 12;43(7):725–31.
5. Yu NC, Raman SS, Kim YJ, Lassman C, Chang X, Lu DSK. Microwave liver ablation: influence of hepatic vein size on heat-sink effect in a porcine model. J Vasc Interv Radiol JVIR. 2008 7;19(7):1087–92. [PubMed: 18589324]
6. Chiang J, Hynes K, Brace CL. Flow-dependent vascular heat transfer during microwave thermal ablation. Conf Proc Annu Int Conf IEEE Eng Med Biol Soc IEEE Eng Med Biol Soc Conf 2012;2012:5582–5.
7. Cuisset T, Beauloye C, Melikian N, Hamilos M, Sarma J, Sarno G, et al. In vitro and in vivo studies on thermistor-based intracoronary temperature measurements: effect of pressure and flow. Catheter Cardiovasc Interv Off J Soc Card Angiogr Interv. 2009 2 1;73(2):224–30.
8. Schutt DJ, Haemmerich D. Effects of variation in perfusion rates and of perfusion models in computational models of radio frequency tumor ablation. Med Phys. 2008;35(8):3462–70. [PubMed: 18777906]
9. Landgraf BR, Johnson KM, Roldán-Alzate A, Francois CJ, Wieben O, Reeder SB. Effect of temporal resolution on 4D flow MRI in the portal circulation. J Magn Reson Imaging JMRI. 2014 4;39(4):819–26. [PubMed: 24395121]
10. Roldán-Alzate A, Francois CJ, Wieben O, Reeder SB. Emerging Applications of Abdominal 4D Flow MRI. AJR Am J Roentgenol. 2016 7;207(1):58–66. [PubMed: 27187681]
11. Roldán-Alzate A, Frydrychowicz A, Niespodzany E, Landgraf BR, Johnson KM, Wieben O, et al. In vivo validation of 4D flow MRI for assessing the hemodynamics of portal hypertension. J Magn Reson Imaging JMRI. 2013 5;37(5):1100–8. [PubMed: 23148034]
12. Owen JW, Saad NE, Foster G, Fowler KJ. The Feasibility of Using Volumetric Phase-Contrast MR Imaging (4D Flow) to Assess for Transjugular Intrahepatic Portosystemic Shunt Dysfunction. J Vasc Interv Radiol. 2018 12 1;29(12):1717–24. [PubMed: 30396843]
13. Committee for the Update of the Guide for the Care and Use of Laboratory Animals; National Research Council. Guide for the Care and Use of Laboratory Animals: Eighth Edition. Washington, D.C.: The National Academies Press; 2010.
14. Loecher M, Ennis DB. Velocity reconstruction with nonconvex optimization for low-velocity-encoding phase-contrast MRI. Magn Reson Med. 2018;80(1):42–52. [PubMed: 29130519]
15. Lu DSK, Raman SS, Vodopich DJ, Wang M, Sayre J, Lassman C. Effect of vessel size on creation of hepatic radiofrequency lesions in pigs: assessment of the “heat sink” effect. AJR Am J Roentgenol. 2002 1;178(1):47–51. [PubMed: 11756085]
16. Chiang J, Willey BJ, Del Rio AM, Hinshaw JL, Lee FT, Brace CL. Predictors of Thrombosis in Hepatic Vasculature during Microwave Tumor Ablation of an In Vivo Porcine Model. J Vasc Interv Radiol JVIR. 2014 9 22; 25(12):1965–1971 [PubMed: 25255704]
17. Chiang J, Martin J, Nickel K, Kimple R, Brace C. Potential mechanisms of the heat-sink effect during microwave ablation of an in-vivo porcine liver model. J Vasc Interv Radiol. 2015 2 1;26(2):S117–8.
18. Meloni MF, Andreano A, Bovo G, Chiarpotto B, Amabile C, Gelsomino S, et al. Acute Portal Venous Injury after Microwave Ablation in an in Vivo Porcine Model: A Rare Possible Complication. J Vasc Interv Radiol JVIR. 2011 5 6; 22(7):947–951 [PubMed: 21550820]
19. Poggi G, Teragni C, Gazzaruso C, Bernado G. Massive hepatic infarction complicating ultrasound-guided percutaneous radiofrequency thermal ablation. Liver Int Off J Int Assoc Study Liver. 2004 12;24(6):704–5.
20. Chiang J, Wang P, Brace CL. Computational modelling of microwave tumour ablations. Int J Hyperth Off J Eur Soc Hyperthermic Oncol North Am Hyperth Group. 2013 6;29(4):308–17.
21. dos Santos I, Haemmerich D, Pinheiro C, da Rocha A. Effect of variable heat transfer coefficient on tissue temperature next to a large vessel during radiofrequency tumor ablation. Biomed Eng OnLine. 2008;7(1):21. [PubMed: 18620566]

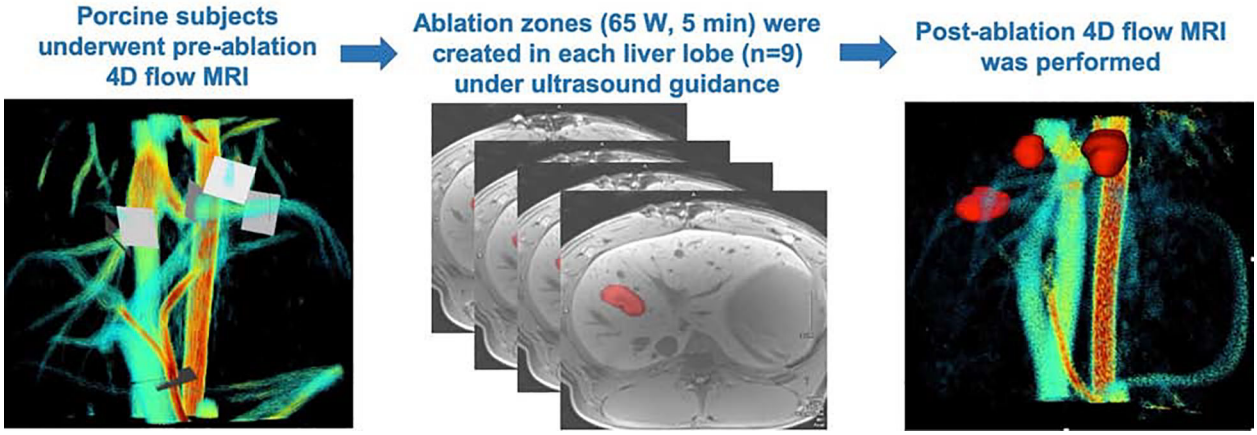

Figure 1.

Workflow of 4D flow MRI and ablation segmentation. 4D flow MRI was performed before and after the microwave ablations were created. Ablation zones volumes were calculated by manual segmentation of the ablation zones. The location of the ablation zones was then registered against the 4D flow data. A post-ablation 4D flow MRI cine can be seen in Video 1.

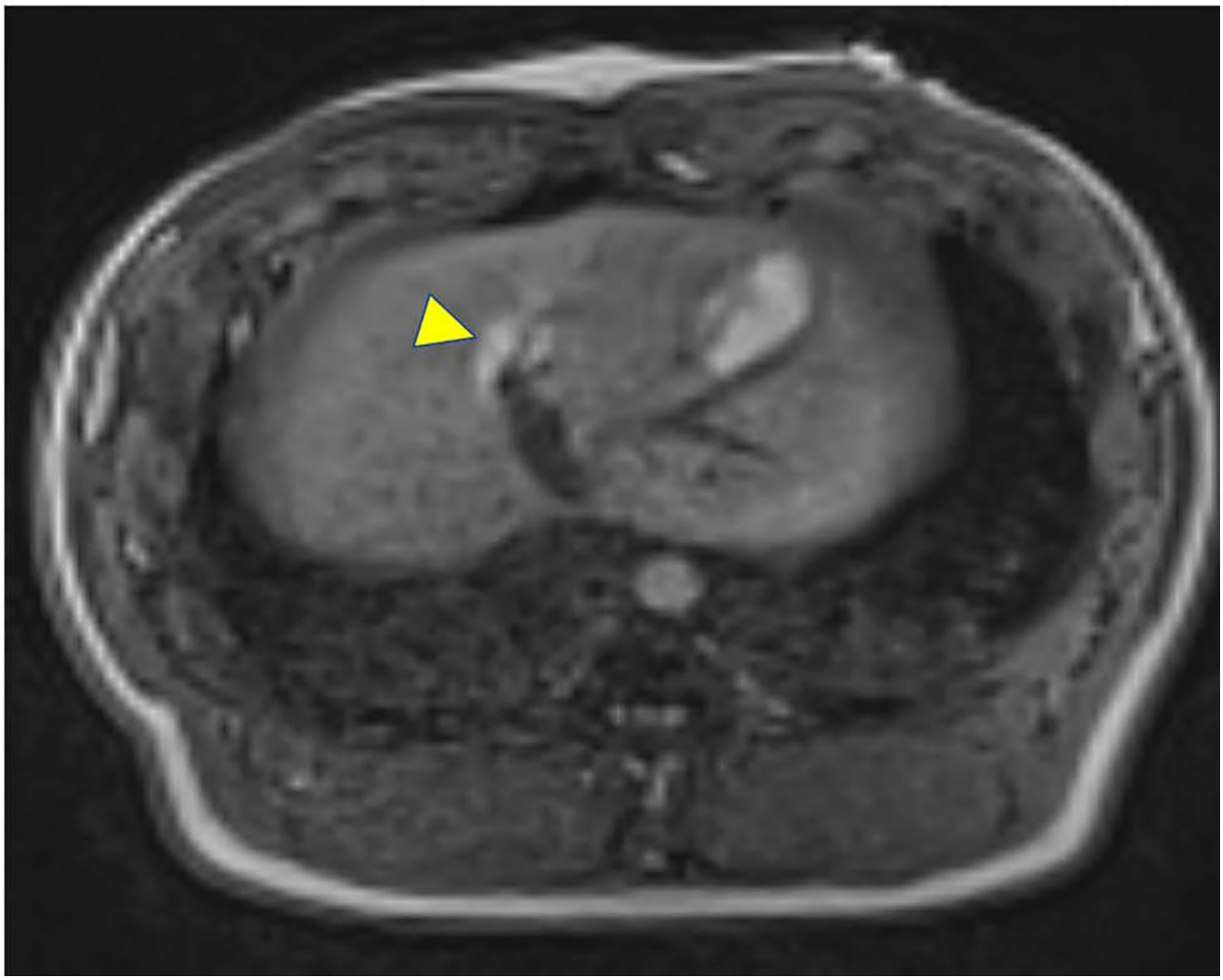

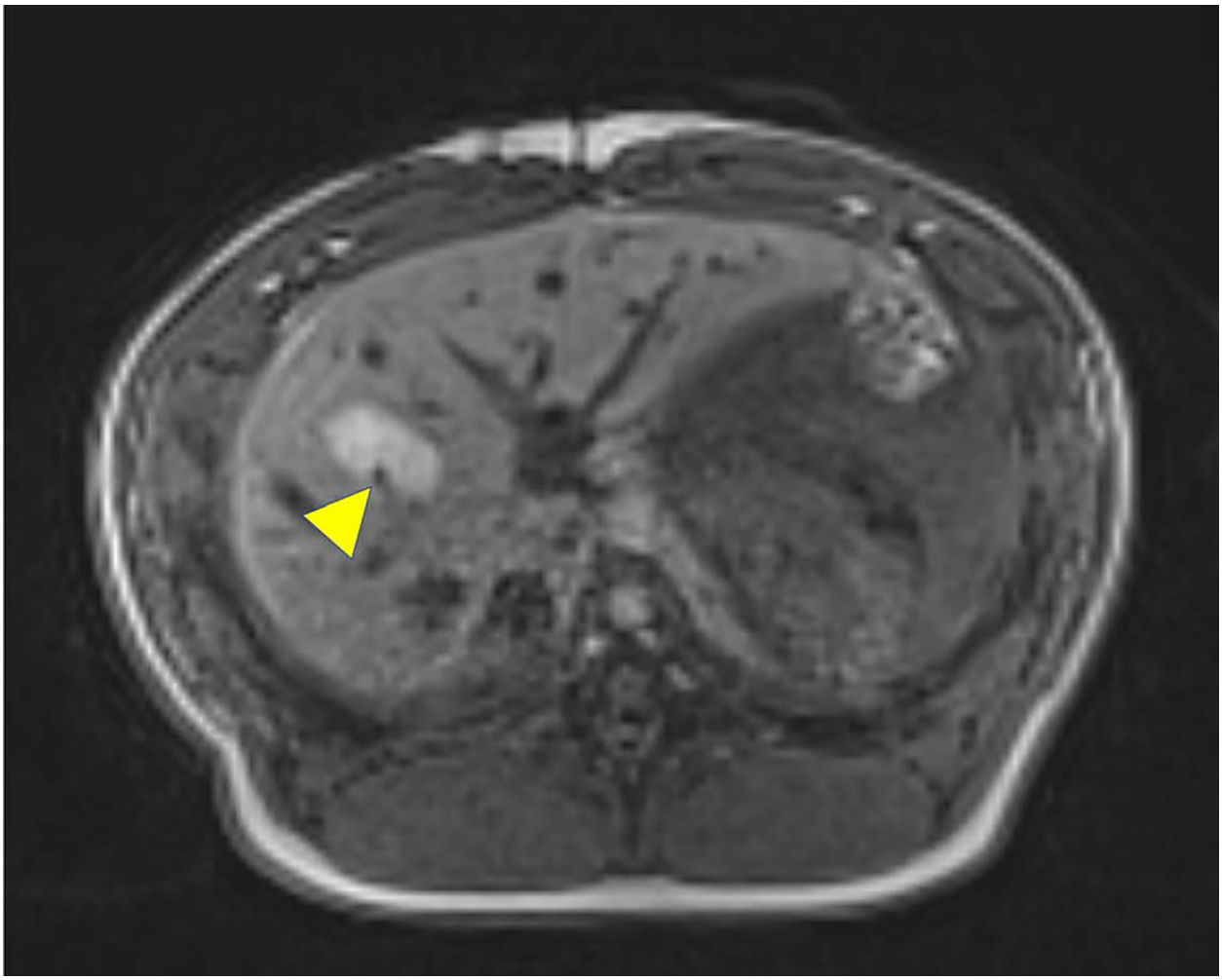

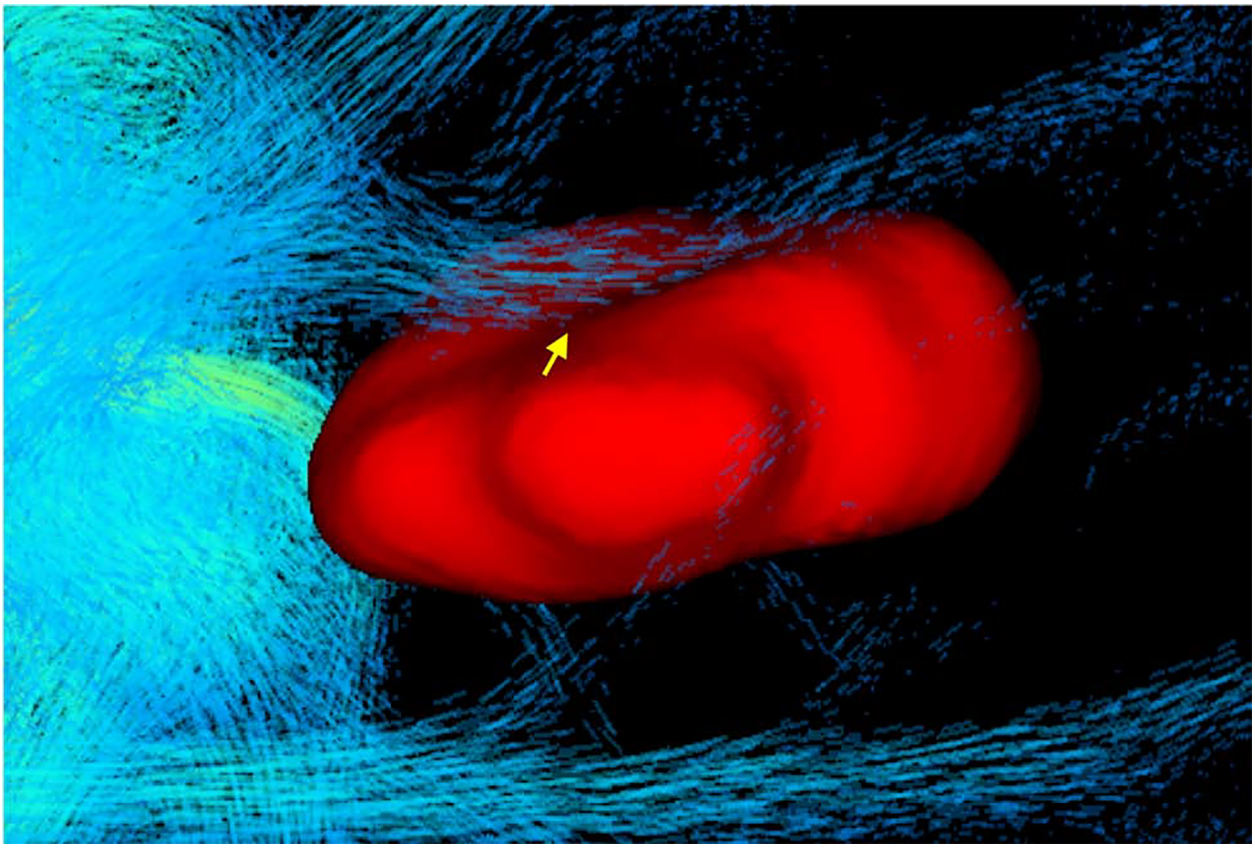

Figure 2.

A) Non-contrast T1-weighted image of a hepatic vein (left) that was completely encompassed by the ablation zone yet remained patent (yellow arrowhead). Note that the hepatic vein appears to contract significantly when it is encompassed in the ablation zone, likely from dehydration and subsequent contraction. B) Non-contrast T1-weighted image of a thrombosed portal vein (yellow arrowhead). Portal veins thrombosed more than hepatic veins (50% vs 0%, p=0.21) and may confer a smaller heat-sink effect compared to hepatic veins. C) 4D flow measurements can quantitatively demonstrate deflection of the ablation zone based on size and velocity measurements of the encased hepatic vein. Note in this image how the hepatic vein deflects the ablation zone (yellow arrow) (Video 2).

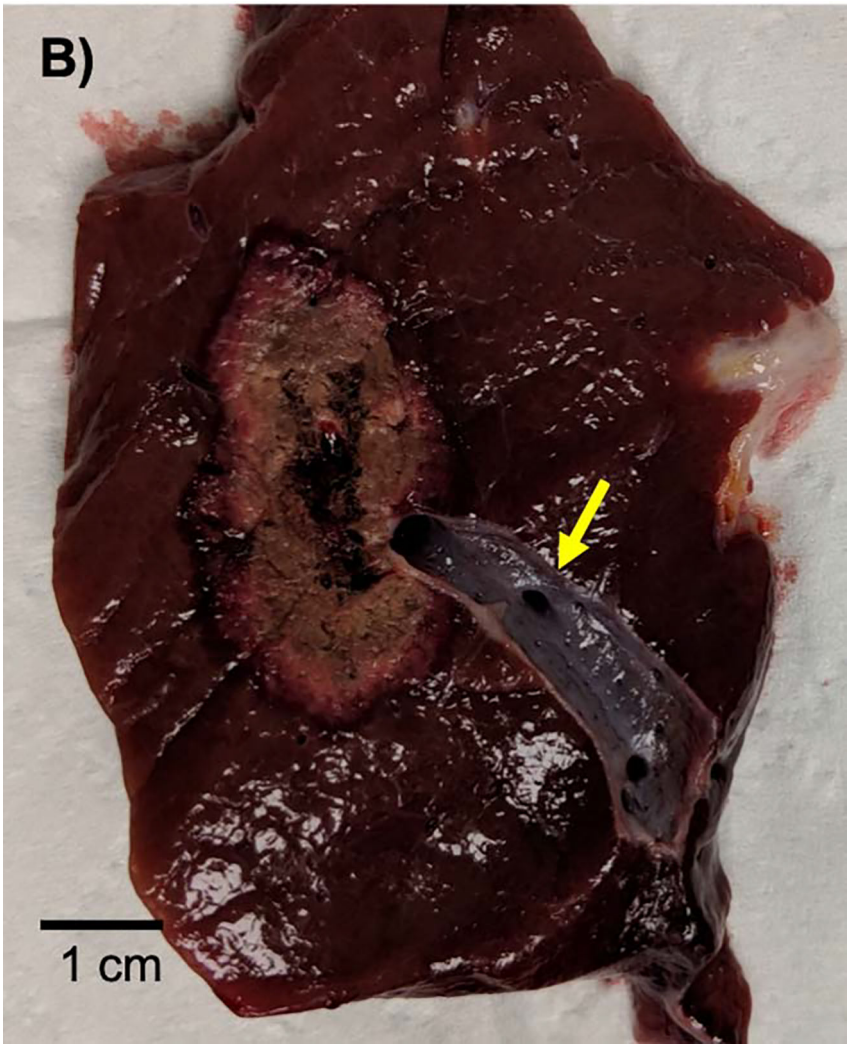

Figure 3.

En-bloc samples of in-vivo liver tissue demonstrating differences in ablation zone sizes based on the vessels nearby. A) Ablation zone that was abutting a portal vein (white arrow), which had thrombosed. The resulting ablation zone measured 4.7 × 3.0 cm in cross sectional dimensions (longitudinal × transverse). B) Ablation zone abutting a hepatic vein (yellow arrow) that remained patent and acted as a persistent heat-sink during the ablation zone that led to a smaller ablation zone, measuring 3.9 × 1.8 cm (longitudinal × transverse).